



Damped least-squares approach for point-source corneal topography

Vyacheslav Sokurenko¹ and Vasyl Molebny^{1,2}

¹National Technical University of Ukraine, Kiev, Ukraine, and ²Institute of Biomedical Engineering, Kiev, Ukraine

Abstract

An optimization algorithm to be used in point-source corneal topographers is developed for the reconstruction of the topography of aspheric corneal surfaces. It is based on the damped least-squares technique. The reconstructions obtained with a topographer comprising 48 or 90 point sources for corneas having different forms (spherical, conicoidal, complex) and apical radii (5–16 mm) were simulated numerically. Zernike polynomials up to the seventh radial order were used for the description of the shape of the anterior corneal surface. With no noise, i.e. uncertainty in the position of the image of each object point, it is shown that this approach allows reconstruction of the surface with a root-mean-square (RMS) error of $<5 \times 10^{-7} \mu\text{m}$ for the elevation map and 3×10^{-7} diopter for the refraction map. With noise, to get an averaged surface elevation RMS error of $<1 \mu\text{m}$, or an averaged refraction RMS error of <0.25 diopter, each spot must be located (in the image plane) with an error $<1 \mu\text{m}$.

Keywords: cornea, elevation map, least squares, point source, refraction map, topography

Introduction

The measurement of corneal topography is of great importance, particularly in the context of contact lenses, refractive surgery and ocular aberration studies. Many current topographic instruments use Placido disk mires, in which the corneal contour is derived from the image of a series of circular rings reflected by the anterior surface of the cornea. Placido disk topographers, however, have a major weakness. They cannot distinguish between distortions in the reflected disk images which result from radial and tangential corneal shape variations. Only radial displacements in the images of points on the edge of each Placido ring can be detected, displacements in the tangential direction being undetected. This is a known skew-ray problem (Rand *et al.*, 1997). Atchison (2006) noted that the skew ray may be

an issue in measurements of ocular aberration when performed with retinoscopy. Iskander *et al.* (2007) have evaluated the significance of the skew ray ambiguity and its effect on the analyzed corneal optics, using a procedure in which they compared the corneal wavefront aberrations estimated from 3D ray tracing with those determined from 2D (meridional based) estimates of the refractive power.

To obtain the required information on the tangential component, the design of the target to be reflected in the cornea must allow image displacement to be measured in both the radial and tangential directions. Projection of a grid pattern was proposed by Warnicki *et al.* (1988) and checkered Placido disks by D'Souza *et al.* (1998). A videokeratoscope based on the imaging of a grid-like pattern was tested by Massig *et al.* (2005). The maximum error of the height data was $<3 \mu\text{m}$, and structures with height deviations of $0.1 \mu\text{m}$ were shown to be easily identifiable. Sicam and Van der Heijde (2006) used a colour-coded stimulus pattern to reconstruct both the rotation-symmetric and non-rotation-symmetric shape features of the anterior corneal surface. In these approaches, the correspondence between the coordinates of the details of the mires and the images of their reflections from the cornea is analyzed. Calculation problems were discussed by Klein (1997). Halstead *et al.*

Received: 8 November 2008

Revised form: 25 January 2009

Accepted: 3 February 2009

Correspondence and reprint requests to: Prof Vasyl Molebny, Presidium of the Academy of Technological Sciences of Ukraine, 42 Acad. Glushkov Prosp., 03187 Kiev, Ukraine.

Tel.: +380 44 524 9164, Fax: +380 44 526 6181.

E-mail address: molebny@mail.ru

(1995) searched for a solution using splines. Molebny *et al.* (2002) proposed a ray-tracing technique to synchronously measure the refractive properties of the optical system of the eye and of its corneal component. This technique used similar algorithms for both calculations, based on polynomial fitting with the least RMS error. Spline fitting for this technique of wavefront and refraction mapping was described by Molebny *et al.* (2008). Sokurenko (2005) outlined a solution for consecutive topography using point sources of light for the case of spherical corneal surfaces. From the construction point of view, an interesting step to the implementation of the point-source approach was made by Ventura *et al.* (2007), who experimented with a keratometric module for a slit lamp containing a circular projection mire using light emitting diodes.

In the present work, we investigate the potential accuracy of an algorithm for the reconstruction of aspheric corneal surfaces which uses information from the reflected images of several concentric sets of circular arrays of point light sources. A special *Keratest* software was developed to simulate the operation of the topographer and to carry out reconstruction of aspheric corneal surfaces. The software is based on an optimization algorithm. Analysis of the accuracy of the algorithm with and without detector noise (i.e. uncertainty in the positions of the reflected images of the object points) is performed when the cornea takes a variety of shapes. Some recommendations are made concerning an appropriate number of Zernike polynomial terms for a topographer with a small number of light sources.

Optimization algorithm for reconstruction of the anterior surface of the cornea

The skew-ray problem is demonstrated in *Figure 1* for an aspheric surface composed of a sphere overlaid with a trefoil component. A projected ring *P*, after reflection from this surface, is imaged as a distorted figure *R*. Some points of the initial ring *P* will be shifted in the image *R* along the radii outward (points 2, 6, 10) or inward (points 4, 8, 12) with regard to the image of the initial ring *P* if it were not distorted. The other points will move tangentially clockwise (points 3, 7, 11) or counter-clockwise (points 1, 5, 9). Significant errors in surface reconstruction can take place if these tangential shifts are not taken into account.

We start by making the general assumption that the object 'mires' consist of a suitable spatial array of point sources and that an image of these as reflected by the cornea is acquired using suitable layout (*Figure 2*). A set of point sources (1, 2, 3, ..., *S*) is positioned in front of an eye. These sources can be installed on a plane or any other kind of a surface, e.g., sphere, cone, ellipsoid, etc.

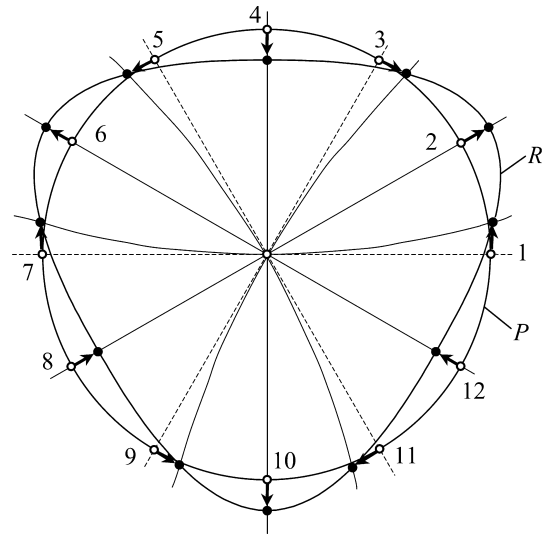


Figure 1. Projected circle *P* and a figure *R* reflected from the cornea. The points on the initial circle *P* are shifted not only in radial direction (points 2, 4, 6, 8, 10, 12), but in the tangential direction as well (points 1, 3, 5, 7, 9, 11).

The light from any of the sources is reflected by the anterior surface of the cornea covered with its tear film. A stop installed in the back focus of the lens selects only the telecentric rays from the reflected beam of light. The sources can be switched on simultaneously or sequentially. With sequential switching, it is easy to avoid any problems with the identification of reflections, which may be especially important for complex surfaces, e.g. in keratoconus.

The algorithm employed for surface reconstruction is based on the damped least-squares method, which is used in optical design software, due to its effective search of local optimum solutions (Kingslake, 1978).

Here, Zernike coefficients describing the form of the anterior cornea are used as the optimization parameters. Let x_i be the i th element of the generalized vector of parameters \mathbf{X} ($i = 1 \dots N$), where N is a total number of optimization parameters. Deviations of the position coordinates of the spot images from given values (computed for the selected model or for one established experimentally in a given topographer system) are used as performance functions f_j , $j = 1 \dots 2S$, where S is the total number of point light sources forming the mire target.

The least-squares solution can be found once the following merit (error) function ξ is minimized:

$$\xi = |\mathbf{F}|^2 = \mathbf{F}^T \mathbf{F},$$

where \mathbf{F} is a $2S$ -element vector of the values f_j , and \mathbf{F}^T denotes the transposed vector \mathbf{F} . In the damped least-squares technique, an optimization follows in repeating iterations (Spencer, 1963):

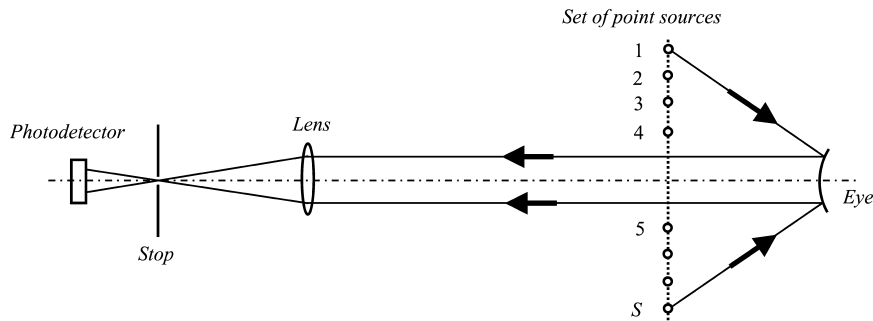


Figure 2. Simplified layout of a point-source topographer. The set of point sources of light can be positioned on a plane surface, as shown, or on the surface of a sphere, cone, ellipsoid, etc.

$$\mathbf{X} = \mathbf{X}_0 - k_l (\mathbf{A}^T \mathbf{A} + p^2 \mathbf{I})^{-1} \mathbf{A}^T \mathbf{F}_0,$$

$$\mathbf{A} = \begin{pmatrix} \frac{\partial f_1}{\partial x_1} & \frac{\partial f_1}{\partial x_2} & \dots & \frac{\partial f_1}{\partial x_N} \\ \frac{\partial f_2}{\partial x_1} & \frac{\partial f_2}{\partial x_2} & \dots & \frac{\partial f_2}{\partial x_N} \\ \dots & \dots & \dots & \dots \\ \frac{\partial f_{2S}}{\partial x_1} & \frac{\partial f_{2S}}{\partial x_2} & \dots & \frac{\partial f_{2S}}{\partial x_N} \end{pmatrix},$$

where \mathbf{X}_0 and \mathbf{X} are the initial and the new vectors of the optimization parameters accordingly, \mathbf{A} is the Jacobian matrix, i.e. a matrix of first partial derivatives of performance functions with respect to optimization parameters; p^2 is the damping factor; \mathbf{I} is the unit diagonal matrix; \mathbf{F}_0 is a vector of performance functions evaluated under initial parameters; and k_l is the factor which defines the length of the descent vector.

An iteration process of optimization is completed once the relative difference ϵ_{rel} (or an absolute difference ϵ_{abs}) of the merit function between each step of the iteration process becomes small enough according to some chosen criterion (Sokurenko, 2005).

The algorithm incorporates real ray tracing through any given optical system with complete ray aiming. In general, the approach can be applied to the optical system of any topographer and the 3D location of light sources can be arbitrarily chosen. For the present study, we consider a lens which is telecentric in the object space.

The anterior surface of the cornea can be described by a set of standard Zernike polynomials up to the seventh order inclusive. The surface is evaluated in terms of the elevation map, i.e. by the deviations (sags) from the plane perpendicular to the optical axis, as well as by the refractive power map in diopters. For the present purposes, analysis is restricted to the area of the corneal zone 10 mm in diameter. Therefore, the normalization radius of the Zernike polynomials is set to 5 mm. The software developed enables estimation of the numerical performance of the algorithm as well as its potential in determining corneal shape with submicron accuracy.

The following data of the topographer system can be varied by a user:

- the total number and location of light sources;
- maximum and minimum object radial heights;
- the radius of curvature and the conic constant of the object surface;
- the object-to-cornea distance;
- the level of noise, simulated as an RMS error of detection of the spot coordinates in the image plane.

An example of a possible arrangement for 90 point light sources in the object surface is shown in *Figure 3*.

Figure 4 demonstrates the results of reconstruction of a complex anterior corneal surface having the defocus coefficient $Z_4 = 0.5$ mm, the primary astigmatism coefficients $Z_3 = -0.2$ mm and $Z_5 = 0.15$ mm as well as the coefficients $Z_6 = 0.04$ mm (oblique trefoil) and $Z_7 = -0.02$ mm (vertical coma). The diameter of the working zone of the cornea (where the reflections occur) for this example is 8.83 mm. *Figure 4a* shows the

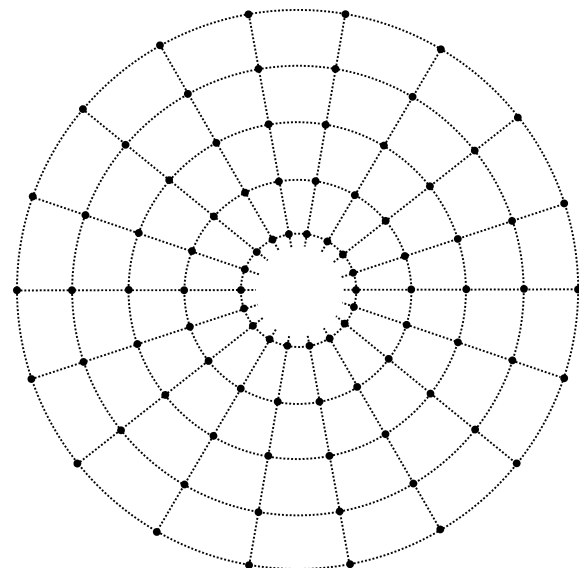


Figure 3. An example of a possible arrangement of light sources at the object surface (as projected on the object plane).

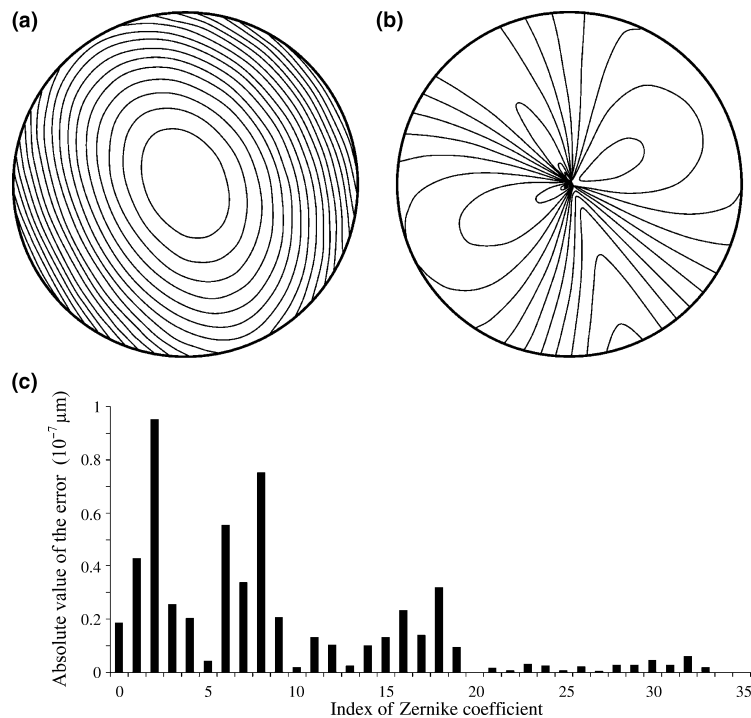


Figure 4. An example of the corneal surface chosen for reconstruction: (a) an elevation map with minimum 0 mm, maximum 1.82 mm, and contour step 0.1 mm; (b) a refraction map with minimum 20 diopters, maximum 65 diopters, and contour step 4 diopters; (c) absolute errors of Zernike coefficient reconstruction. In this case it has been assumed that there is no uncertainty (noise) in the positions of the point images.

corneal elevation map and *Figure 4b* the corresponding refractive map. The array of point sources shown in *Figure 3* is imaged by reflection from the tested surface. For this example, the positions of light spots at the photodetector plane are shown on the spot diagram in *Figure 5*. Reconstruction from these positional data results in very small discrepancies between the original and recalculated Zernike coefficients, as shown in *Figure 4c*.

In another example ($Z_4 = 0.47$ mm, $Z_5 = 0.15$ mm), we compared the accuracy of surface reconstruction with Placido-disk and point-source techniques. It is evident from *Figure 6* that the reconstruction error of the Zernike coefficients with the point-source technique is, at least in principle, 7–9 orders lower than with the Placido-disk technique, which does not take into account the tangential shifts of the image points. The main benefit of this technique for clinicians will be that the true results of corneal examination can be acquired with a high accuracy consistent with the accuracy of wavefront instruments.

Numerical simulation

To estimate the potential accuracy of the developed algorithm, a series of computer experiments was performed to study the results given when the approach was applied to different shapes of the cornea. The basic form

of the cornea was either spherical, conicoidal or complex (specified in terms of the corresponding Zernike coefficients).

In the statistical computations, the initial surfaces had the following range of parameters:

- for spherical surfaces: radii of curvature from 5 to 16 mm;
- for conicoidal surfaces: an apex radius from 5 to 16 mm, an asphericity parameter (conic constant) between -5 and 5 ;
- for complex surfaces, described by Zernike polynomials: coefficient $Z_4 = 0.2 \dots 1$ mm that corresponds approximately to a radius of curvature of the cornea from 5 to 16 mm; the values of other coefficients were in the range from $-0.1/R^n$ to $0.1/R^n$ mm, where R is a normalization radius and n is a radial order of a Zernike coefficient.

Note that the values taken for corneal radii covered a much wider range than that found in normal human corneas (7–9 mm) but it was desirable to check that the algorithm remained well-behaved over the larger range.

Random values for the parameters of an initial model were generated with an equal probability within the ranges defined by the minimum and maximum values. The order-by-order optimization strategy was applied for each examination up to the seventh radial order.

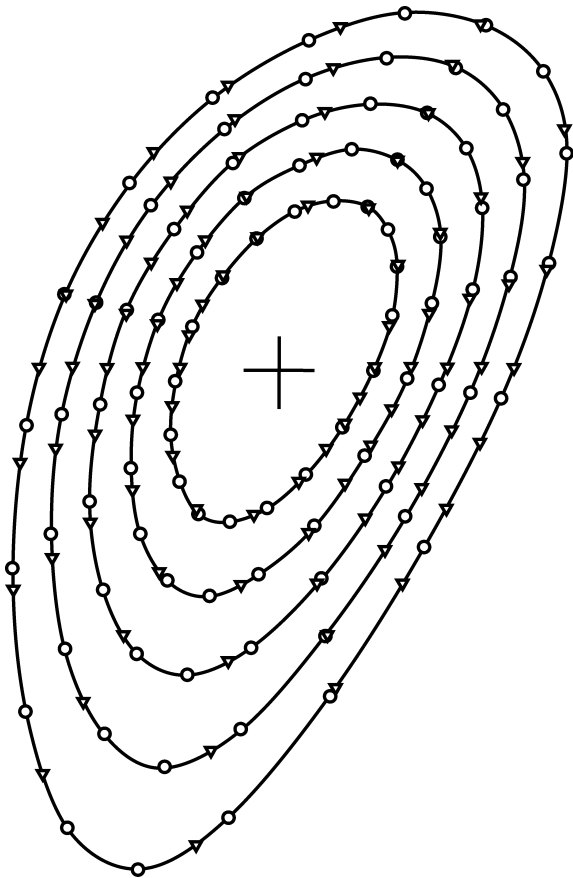


Figure 5. Spot diagram (position of light spots) in the image plane. Circles indicate spot positions in the point-source topographer and triangles indicate the positions that would be detected in the Placido-disk topographer. The maximum displacement in the vertical or horizontal direction is 1.54 mm (see text for details).

Surface elevation, as well as refractive power errors, are displayed in the form of maps reconstructed with the resolution 256×256 samples, the pupil 10 mm in

diameter being inscribed in these 256×256 samples. The simulated pupil zone is located inside this 10 mm circle. The term ‘averaged’ means an averaged value, obtained over all realizations.

Refractive power values are calculated using real ray-tracing of the corneal surface for an axial object point located at infinity. Therefore, due to its aberrational properties, even a pure spherical surface has a non-zero refraction power range (approximately from 0.5 to 1.9 diopters when the corneal surface radius varies from 16 to 5 mm). To decrease the duration of the surface reconstruction process, a reverse ray-tracing procedure was applied. This avoided a time-consuming subroutine for evaluating real apertures (ray aiming) for each light beam.

We investigated the accuracy of surface reconstruction as a function of the total number of point sources (48 or 90) with noise levels from 0 to 2 μm . We did not care about the origins of noise: these could be the errors of measurement of spot coordinates at the photodetector plane due to speckle structure of light, sensor pixelation, and aberrations in the optical system, or might arise from the positioning of the light sources, detector noise itself, etc. We treated all sources of noise as an equivalent uncertainty in the determination of coordinates of the image points. At reconstruction, Zernike polynomials were used up to the seventh radial order inclusive. The results of the simulations are presented in *Table 1* where the RMS values are averaged over 100 realizations.

It can be seen that potential accuracy (with no noise) is better than 5×10^{-7} mm for the elevation map and 3×10^{-7} diopters for the refraction map accordingly. These results do not change critically when the number of point sources for spherical and conicoidal surfaces is varied. For complex surfaces, the considerable influence of noise is observed, with RMS errors increasing

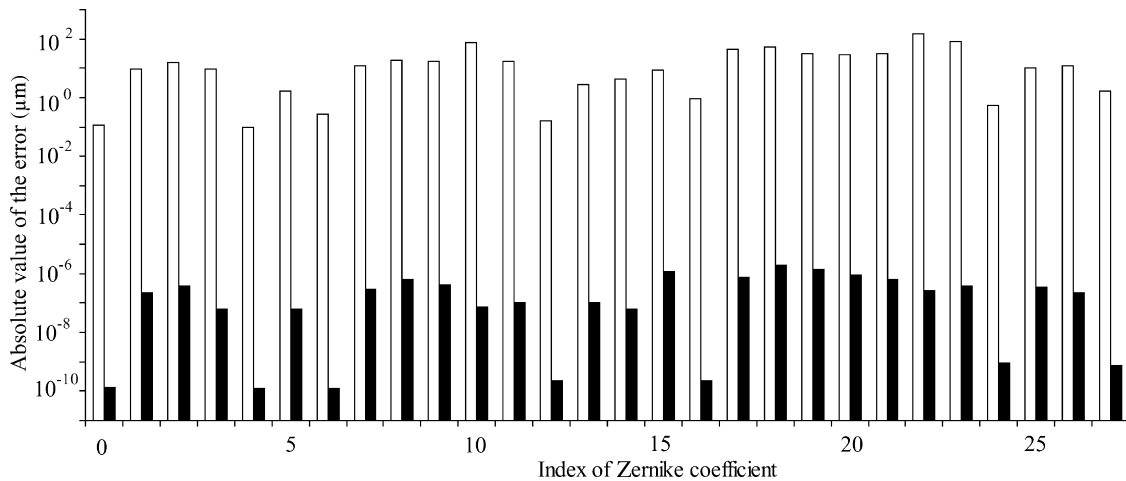


Figure 6. Absolute value of the error of elevation reconstruction with point-source technique (filled bars) in comparison with any other technique (e.g. Placido disk), which does not take into account the tangential shifts in the image reflected from the cornea (white bars).

Table 1. Dependence of the sag errors of surface reconstruction on the number of point light sources used and on the level of RMS noise in the measurement of the positions of the images of the point sources

Spot coordinate RMS error at the image plane (μm)	Surface sag RMS error for the anterior corneal surface (μm)					
	Spherical		Conicoidal		Complex (described by Zernike coefficients)	
	48 sources	90 sources	48 sources	90 sources	48 sources	90 sources
0.0	7.9×10^{-4}	7.3×10^{-4}	2.5×10^{-2}	1.7×10^{-2}	1.4×10^{-6}	4.5×10^{-7}
0.5	0.29	0.24	0.21	0.24	1.83	1.21
1.0	0.63	0.71	0.53	0.34	3.11	2.75
2.0	1.53	1.06	1.02	1.01	6.98	3.96

substantially even for low levels of noise. In the second series of trials, we investigated the accuracy of the corneal surface reconstruction as a function of maximum radial order for the Zernike polynomials used.

The results of simulations with three types of surface under different levels of noise in the measured positions of the point images (RMS errors from 0 to 2 μm) are presented in the graphs of Figure 7. With no noise, the increase of the maximum radial order results in the decrease of the elevation RMS error to 7.3×10^{-4} mm for spherical surfaces; to 0.026 mm for conicoidal

surfaces, and to 1.7×10^{-7} mm for complex surfaces described by Zernike polynomials.

Under the conditions as described, use of Zernike polynomials up to and including the sixth maximum radial order was found to be optimal for surface reconstruction from the standpoint of minimization of the averaged elevation RMS error in the presence of the detector noise (see Figure 7 where in 7a and 7b errors increase slightly when the seventh Zernike order is included). Similar conclusions were reached by Iskander and Collins (2001) and Sicam *et al.* (2004).

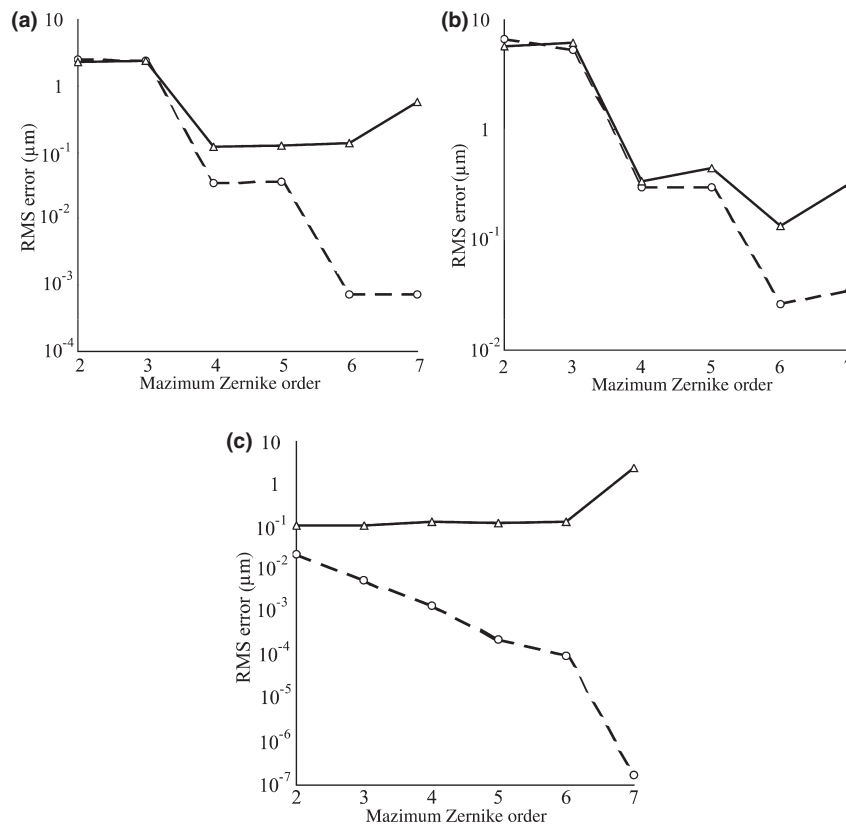


Figure 7. Averaged elevation (sag) RMS error in dependence on maximum Zernike order. Circles correspond to the surfaces without noise and triangles are obtained under an RMS noise level of 1 μm in the positions of the point images: (a) pure spherical surfaces; (b) conicoidal surfaces; (c) complex surfaces.

Table 2. RMS errors in the estimated radius of curvature of the apex of a spherical surface as a function of the RMS errors in point-image position and the number of Zernike coefficients used in the reconstruction

Maximum radial order of Zernike polynomials	Simulated RMS error of measurement of light spot coordinates (μm)			
	0	0.5	1	2
	RMS error of calculated radius of curvature (μm)			
2	0.43	0.41	0.39	0.41
3	0.42	0.42	0.41	0.4
4	1.82×10^{-2}	1.81×10^{-2}	1.76×10^{-2}	1.87×10^{-2}
5	1.75×10^{-2}	1.77×10^{-2}	1.69×10^{-2}	1.79×10^{-2}
6	7.4×10^{-4}	3.32×10^{-3}	6.42×10^{-3}	1.51×10^{-2}
7	7.3×10^{-4}	3.55×10^{-3}	7.69×10^{-3}	1.3×10^{-2}

The accuracy with which the radius of curvature of spherical surfaces could be reconstructed was also explored. Results of these numerical simulations are shown in *Table 2*. As can be seen, even when the image is distorted by noise (with spot coordinate measurement error $2 \mu\text{m}$), the RMS error of apex radius reconstruction does not exceed $0.02 \mu\text{m}$ when the maximum radial order of Zernike polynomials is four through seven.

Conclusions

(1) In general, the results of the numerical investigations of the algorithm outlined in this paper prove its efficiency in the reconstruction of complex aspheric corneal surfaces having no axial symmetry. The approach as applied to point-source topography overcomes the problems of detecting tangential image displacements that are inherent in Placido disk topographers and offers considerable promise for the development of improved instrumentation for determining corneal topography. With no noise, even for a small number (48) of light sources the RMS error of reconstruction of complex surfaces, which are described by Zernike polynomials up to the seventh radial order, is $< 5 \times 10^{-7} \mu\text{m}$ for the elevation map and 3×10^{-7} diopter for the refraction map. The developed algorithm ensures that the averaged elevation fitting RMS error is not $> 0.025 \mu\text{m}$ and the refraction power RMS error < 0.02 diopter for all the corneal surface models considered.

(2) Errors in spot position measurement (noise) have a substantial impact on the accuracy of corneal surface reconstruction. In particular, to achieve an averaged surface elevation RMS error $< 1 \mu\text{m}$, the spot position RMS error at the image plane should not be $> 5 \mu\text{m}$ for purely spherical surfaces and $1 \mu\text{m}$ for conicoidal surfaces. For purely spherical surfaces, the averaged refraction RMS error of 0.25 diopter requires spot positions to be measured with an RMS error $< 1 \mu\text{m}$.

(3) It was numerically proved that complex surfaces can be reconstructed with extremely high accuracy if there is no noise. Complex surfaces are 3–20 times more sensitive to spot measurement noise than are spherical or conicoidal surfaces (see *Table 1*). The conicoidal model is the most robust against measurement noise.

(4) For purely spherical corneal surfaces, the RMS error of apex radius reconstruction is $< 8 \times 10^{-4} \mu\text{m}$ with no noise. It does not exceed $0.013 \mu\text{m}$ when the RMS error of light spot position measurement is $2 \mu\text{m}$.

(5) Six radial orders of Zernike polynomials result in higher accuracy than seven orders (for a point-source topographer with < 100 light points when $1 \mu\text{m}$ noise is involved).

(6) Further investigation is to be carried out to estimate the optimal 3D locations of the point sources, the influence of errors caused by a topographer alignment, and the limitations of the algorithm in the reconstruction of extremely complex corneal surfaces.

Acknowledgement

The authors thank Professor W. N. Charman for his care and professional help in the process of preparation of this work for publication.

Financial interest

None.

References

- Atchison, D. A. (2006) The skew ray issue in ocular aberration measurement. *Optom. Vis. Sci.* **83**, 396–398.
- D'Souza, H. M., Sarver, E. J. and Wakil, Y. S. (1998) Method of corneal analysis using a checkered Placido apparatus. U.S. Patent 5,841,511.
- Halstead, M. A., Barsky, B. A., Klein, S. A. and Mandell, R. B. (1995) A spline surface algorithm for reconstruction of corneal topography from a videokeratographic reflection pattern. *Optom. Vis. Sci.* **72**, 821–827.
- Iskander, D. R. and Collins, M. J. (2001) Optimal modeling of corneal surfaces with Zernike. *IEEE Trans. Biomed. Eng.* **48**, 87–95.
- Iskander, D. R., Davis, B. A. and Collins, M. J. (2007) The skew ray ambiguity in the analysis of videokeratoscopic data. *Optom. Vis. Sci.* **84**, 435–442.
- Kingslake, R. (1978) *Lens Design Fundamentals*. Academic Press, San Diego.
- Klein, S. A. (1997) Corneal topography reconstruction algorithm that avoids skew ray ambiguity and the skew ray error. *Optom. Vis. Sci.* **74**, 945–962.
- Massig, J. H., Lingelbach, E. and Lingelbach, B. (2005) Videokeratoscope for accurate and detailed measurement of the cornea surface. *Appl. Opt.* **44**, 2281–2287.

- Molebny, V., Pallikaris, I., Wakil, Y. and Molebny, S. (2002) Method and device for synchronous mapping of the total refraction non-homogeneity of the eye and its refractive components. U.S. Patent 6,409,345.
- Molebny, S., Molebny, V. and Laster, L. (2008) Method for measuring the wave aberrations of the eye. U.S. Patent 7,380,942.
- Rand, R. H., Howland, H. C. and Applegate, R. A. (1997) Mathematical model of a Placido disk keratometer and its implications for recovery of corneal topography. *Optom. Vis. Sci.* **74**, 926–930.
- Sicam, V., Coppens, J., Van den Berg, T. and Van der Heijde, R. (2004) Corneal surface reconstruction algorithm that uses Zernike polynomial representation. *J. Opt. Soc. Am. A* **21**, 1300–1306.
- Sicam, V. A. and Van der Heijde, R. G. (2006) Topographer reconstruction of the nonrotation-symmetric anterior corneal surface features. *Optom. Vis. Sci.* **83**, 910–918.
- Sokurenko, V. M. (2005) The method of consecutive corneal topography. *Her Kiev Polytechnic Inst., Instrum. Ser.* **29**, 94–102.
- Spencer, G. H. (1963) A flexible automatic lens correction procedure. *Appl. Opt.* **2**, 1257–1264.
- Ventura, L., Riul, C. and De Faria e Sousa, S. J. (2007) Optical projection mires for measurements of the radii of curvature of the cornea in biomicroscopes. *Appl. Opt.* **46**, 7155–7161.
- Warnicki, J. W., Rehkopf, P. G., Curtin, D. Y., Burns, S. A., Arffa, R. C. and Stuart, J. C. (1988) Corneal topography using computer analyzed rasterstereographic images. *Appl. Opt.* **27**, 1135–1140.